Available online at www.sciencedirect.com
ScienceDirect
ELSEVIER
International Journal of Pharmaceutics 331 (2007) 197–203
INTERNATIONAL JOURNAL OF PHARMACEUTICS
www.elsevier.com/locate/ijpharm

Pharmaceutical Nanotechnology

Colloidal stability of ultrasmall superparamagnetic iron oxide (USPIO) particles with different coatings

Mariagrazia Di Marco [a,b,*], Irene Guilbert [b], Marc Port [b], Caroline Robic [b], Patrick Couvreur [a], Catherine Dubernet [a]

[a] *Univ Paris Sud XI, UMR CNRS 8612, 5 Rue JB Clément, 92926 Châtenay Malabry, France*
[b] *Guerbet, Centre de Recherche BP 57400, 95943 Roissy CdG Cedex, France*

Received 11 August 2006; accepted 25 October 2006
Available online 3 November 2006

Abstract

Ultrasmall superparamagnetic iron oxide (USPIO) particles are efficient contrast agents used in vivo to enhance relaxation differences between healthy and pathological tissues. Detailed understanding of their physicochemical properties in suspension is necessary to guarantee the quality and safety of biological USPIO particles application. The ferrofluids stability against aggregation and gravitational settling affects their biodistribution and consequently the resulting contrast. In this study, the stability of iron oxide particles was investigated by dynamic light scattering (DLS) at different NaCl concentrations in order to monitor the evolution of the hydrodynamic radius of the particles with time. The results were interpreted using the classical DLVO theory of colloidal stability. The electrophoretic mobility and the models generally used to convert it to zeta potential were discussed and related to the stability results.

Keywords: Aggregation; Contrast agents; Colloidal stability; Iron oxide; Nanoparticles; Size

1. Introduction

Magnetic nanoparticles suspensions (ferrofluids) are becoming increasingly important for biomedical applications (Halbreic et al., 1998). We focused on the physicochemical aspects of ultrasmall superparamagnetic iron oxide (USPIO) particles intended for magnetic resonance imaging (MRI) purposes (LaConte et al., 2005). These small particles (γ-Fe_2O_3), that exhibit superparamagnetism and high saturation magnetization values (Chatterjee et al., 2003), are used as contrast agents to enhance relaxation differences between healthy and pathological tissues. Intravenous administration of the USPIO is the most convenient way to target organs and tissues, since all vital cells receive supplies by means of the blood circulation. However, in order to make the particles delivery efficient and to improve their vascular permanence, the particle surface needs to be modified to minimize or delay the nanoparticles uptake by the mononuclear phagocyte system (MPS or reticuloendothelial system) (Moghimi et al., 2001; Mornet et al., 2004). Nanoparticles showing the longest plasma half-life generally have a small size, neutral and hydrophilic surface. Therefore, the particle surface properties, which control the stability of the ferrofluids against aggregation phenomena, have an important role in the transport and biodistribution resulting efficient contrast agents (Pouliquen et al., 1992; Guptaa and Gupta, 2005; Tartaj et al., 2005).

In order to prevent particles aggregation due to attractive van der Waals or magnetic dipole–dipole interactions a repulsive force between particles may be created by means of steric or electrostatic repulsion. An interesting approach to the determination of electrostatic and steric stabilization mechanism of the colloidal particles is based on following their aggregation kinetics by varying the salt concentration.

The major difficulties encountered in the physicochemical study of USPIO particles are due to their small dimensions. According to our knowledge a similar study, applied to particles in the 100 nm range, was not previously described with so tiny particles (hydrodynamic radius R_H around 12 nm). Our purpose was hence to suggest an experimental procedure that could help determine the contribution of different coatings to the stabilization of ultra small iron oxide nanoparticles. The stability

* Corresponding author. Tel.: +33 677798374.
E-mail address: mariagraziad@gmail.com (M. Di Marco).

0378-5173/$ – see front matter © 2006 Elsevier B.V. All rights reserved.
doi:10.1016/j.ijpharm.2006.11.002

of iron oxide particles in the presence of NaCl was studied by dynamic light scattering, following the particle radius with time. The results were interpreted using the classical DLVO theory (Derjaguin and Landau, 1941; Vervey and Overbeek, 1948) of colloidal stability, extended to take in account hydration effects. Electrophoretic mobility was determined and the models generally used to convert it to zeta potential were discussed.

2. Materials and methods

2.1. Nanoparticles characterization

Superparamagnetic iron oxide nanoparticles (maghemite) were synthesized via aqueous precipitation of magnetite, according to a previously reported method (Port et al., 2004), and followed by an oxidation to maghemite under acid conditions. The ferrimagnetic fine particles were then coated with different types of organic layers in order to prevent colloidal coagulation. Particles were purified by ultrafiltration. Colloids were considered as ready to use and contaminant-free when the conductivity of the supernatant liquid after ultrafiltration was close to that of deionised water. Table 1 shows the kind of coatings investigated in our experiments: five samples including the reference (particles only electrically stabilized by carboxylates), two different adsorption densities of a low molecular weight amino-alcohol derivative of glucose (MW ca. 330) and two PEG chains varying by their length (MW ca. 750 and 2000). The iron core and the coating content of the γ-Fe_2O_3 nanoparticles in aqueous suspension were determined, respectively, by Inductively Coupled Plasma Atomic Emission Spectrophotometry (ICP-AES) using a Varian Liberty 150 and elemental analysis of the organic compounds.

2.2. Colloid aggregation kinetics

Colloidal particles randomly collide with each other at a rate determined by their Brownian motion. The rate of particle collision in a suspension is therefore diffusion limited and is proportional to the suspension concentration and temperature. The collision can result in the formation of an aggregate if the particles remain in contact after the encounter. The stability ratio W of colloidal system is commonly expressed by (Holthoff et al., 1996):

$$W = \frac{k_{\text{fast}}}{k} \tag{1}$$

Table 1
Examined coatings and % of surface binding sites occupied

Kind of coating	% of surface occupied binding sites
Reference	–
Amino-alcohol100	100
Amino-alcohol86	86
PEG750	60
PEG2000	50

where the rate constant k_{fast} describes rapid aggregation (all collisions result in aggregation) and k is the rate constant for slow aggregation state (only a fraction of the collisions results in aggregation). When $W>1$ only a fraction of the collisions leads to aggregates because of the presence of an energy barrier generated by the sum of the attractive and repulsive forces acting between the particles. Aggregation occurring when the energy barrier is not sufficiently high to completely stabilize the suspension is named 'slow'. When $W=1$ every collision produces an aggregate (lack of the energy barrier) and the diffusion limited aggregation rate (fast) occurs. Our purpose is to determine the stability W ratio of the different USPIO suspensions. In this work, the rate constant of coagulation W was measured by monitoring the increase in R_{H} with time at different salt concentrations using dynamic light scattering (Schudel et al., 1997):

$$\left(\frac{\mathrm{d}R_{\text{H}}}{\mathrm{d}t}\right)_{t\to 0} \propto k n_0 \tag{2}$$

Actually the slope of the R_{H} versus time curve for $t \to 0$ at each salt concentration is proportional to the product of the aggregation rate constant k and the colloid number concentration n_0. When n_0 is kept constant from one experiment to another, the stability ratio W is proportional to k_{fast}/k and can be simply given by the ratio of the initial slopes of the R_{H} versus time curves:

$$W = \frac{(\mathrm{d}R_{\text{H}}/\mathrm{d}t)_{t\to 0\,\text{fast}}}{(\mathrm{d}R_{\text{H}}/\mathrm{d}t)_{t\to 0}} \tag{3}$$

Thus, Eq. (3) was used for the experimental determination of the stability ratio W of the iron oxide suspensions by simply dividing the initial slopes (estimated with low-order polynomial fitting) of the R_{H} versus time curves for the fast and the slow region of coagulation. The stability ratio W, previously introduced as the ratio between rapid and slow aggregation rates, depends on the total interaction energy (or energy barrier) $V_{\text{T}}(H)$ and their relation is defined by the following equation (Puertas and de las Nieves, 1999):

$$W = \frac{\int_0^\infty \beta(H)/(H+2a)^2 \, \exp(V_{\text{T}}(H)/K_{\text{B}}T)\,\mathrm{d}H}{\int_0^\infty \beta(H)/(H+2a)^2 \, \exp(V_{\text{A}}(H)/K_{\text{B}}T)\,\mathrm{d}H} \tag{4}$$

where H is the distance between the particle surfaces, $\beta(H)$ the hydrodynamic correction factor (Overbeek, 1982), a the radius of the spherical particles, $V_{\text{A}}(H)$ the potential energy of the van der Waals interaction and $V_{\text{T}}(H)$ is the total potential energy of interaction.

The total interaction energy between the particles $V_{\text{T}}(H)$ is given by the sum of the van der Waals $V_{\text{A}}(H)$ and the electrostatic double layer $V_{\text{E}}(H)$ interaction energy (DLVO theory):

$$V_{\text{T}}(H) = V_{\text{A}}(H) + V_{\text{E}}(H) \tag{5}$$

The van der Waals interaction is given by:

$$V_{\text{A}}(H) = -\frac{A}{6}\left[\frac{2a^2}{H(4a+H)} + \frac{2a^2}{(2a+H)^2} + \ln\frac{H(4a+H)}{(2a+H)^2}\right] \tag{6}$$

where A is the Hamaker constant of particles interacting in the medium (water). The repulsive interaction between the electrical

double layers of the particles, $V_E(H)$, is given by:

$$V_E(H) = 2a\varepsilon_0\varepsilon_r\pi\left(\frac{4K_BT}{ze}\gamma\right)^2 e^{-\kappa H} \quad (7)$$

with

$$\gamma = \frac{e^{ze\psi_d/2K_BT} - 1}{e^{ze\psi_d/2K_BT} + 1} \quad (8)$$

where κ is the Debye parameter referred as the reciprocal of the double-layer thickness which depends on the ionic strength of the solution, ε_0 the permittivity in vacuum, ε_r the relative permittivity. z the valence of the electrolyte, K_B the Boltzmann constant, T the absolute temperature and ψ_d is the diffusion potential that may be very close to the zeta potentials (ζ) (Ortega-Vinuesa et al., 1996; Kobayashi et al., 2005). The determination of A and ψ_d by fitting procedure also allows estimating the energy barrier of the colloidal system. Our purpose was then to use this procedure to compare the barrier levels of the different USPIO coatings. The procedure consisted in fitting the experimental points of log W versus electrolyte concentration by Eq. (4), using the Hamaker constant (A) and the potential of diffusion (ψ_d) as fitting parameters. The fitting procedure followed the Levenberg–Marquardt method (general last square fitting).

2.3. Particle size analysis

The particle size was measured in different conditions (varying salt concentration) by dynamic light scattering (DLS) performed on a Malvern 4700 system (Malvern Instruments, UK). NaCl was used as electrolytes for all the samples and $CaCl_2$ for the NaCl stable samples. All measurements were performed at 20 °C with the scattering angle fixed at 90°. Colloid coagulation was started by adding to the electrolyte solutions, in the light scattering cell, an appropriate amount of iron oxide suspension (initial concentration varying between 0.2–0.4 mol/l Fe depending on the batches) to have the same n_0 concentration in each experiment (Schudel et al., 1997). The resulting dispersion, after a quick shake, was then placed in the index matching vat. Individual autocorrelation functions were successively acquired over a period of 1–2 h. The lower limit of the temporal resolution for a given sample is determined by the time necessary to obtain an autocorrelation function with sufficient statistical accuracy. Considering that the initial particle size (R_H) was uniformly distributed around 12 nm, the calculated values obtained along the time represented a mean hydrodynamic radius, R_H, taken over a distribution of colloid monomers, dimers, and higher order aggregates.

2.4. Electrophoretic mobility and zeta potential

The determination of the electrophoretic mobility μ was carried out as function of ionic strength with a Malvern Zetasizer nano ZS90 (Malvern Instruments, UK) using the Universal Dip Cell, guarantying the absence of any chemical incompatibility with the iron oxide nanoparticles sample. The measures were performed by the Cumulant method (monomodal) applying a voltage of 4 V. The optimal frequency and voltage had to be previously determined to minimize particles denaturation. The literature reports several electrophoretic mobility formulas which relate the electrophoretic mobility to the zeta potential of a particle (Kuo and Lin, 2006). The electrophoretic mobility μ of a spherical colloidal particle of radius a, carrying low zeta potential, ζ, and moving in an electrolyte solution, is given by Henry formula valid when the particle surface can be considered locally planar (without any surface structures):

$$\mu = \frac{\varepsilon_0\varepsilon_r}{\eta}\zeta f(\kappa a) \quad (9)$$

with

$$f(\kappa a) = \{1 - e^{\kappa a}[5E_7(\kappa a) - 2E_5(\kappa a)]\} \quad (10)$$

where $f(\kappa a)$ is Henry's function, $E_n(\kappa a)$ the nth order exponential integral, ε_r and η, respectively, the relative permittivity and the viscosity of the electrolyte solution, ε_0 the permittivity in vacuum and κ is the Debye–Hückel parameter.

Only when $\kappa a \to \infty$, $f(\kappa a)$ tends to unity so that Eq. (9) becomes the most widely employed Smoluchowski formula shown below:

$$\mu = \frac{\varepsilon_0\varepsilon_r}{\eta}\zeta \quad (11)$$

while when $\kappa a \to 0$, $f(\kappa a)$ tends to 2/3 and Eq. (9) becomes Hückel formula.

Therefore, the users have to carefully select the appropriate model to convert the electrophoretic mobility values to zeta potential. Moreover, most of the colloidal nanoparticles used for pharmaceutical purpose are coated and cannot really be considered as having a locally planar surface. In order to take into account this parameter, Ohshima proposed a soft particle model by combining the theory of rigid spherical colloids with the theory of completely permeable polyelectrolytes or polymer (Ohshima, 1995). The Ohshima equation tends to Henry mobility formula in the absence of polymer layer. This theoretical survey clearly emphasizes that zeta potential values strongly depend on the equation chosen to convert the electrophoretic mobility to zeta potential. Our particles (very small, strongly negative, and coated) are not really suitable for anyone of these theories and misuse of them could lead to artifacts.

In the present work, the surface properties of iron oxide nanoparticles were directly compared using the electrophoretic mobility data, combining the values obtained in various ionic strengths.

3. Results and discussion

The particle mean radius was determined by dynamic light scattering as function of ionic strength for all samples in order to estimate the particle colloidal stability. As shown in Fig. 1 for the reference sample and in Fig. 2 for one of the amino-alcohol-coated nanoparticles (that at higher percentage of surface binding sites occupied), the hydrodynamic radius R_H increases with time depending on salt concentration. In contrast, the PEG-coated particles were stable over the whole range of salt

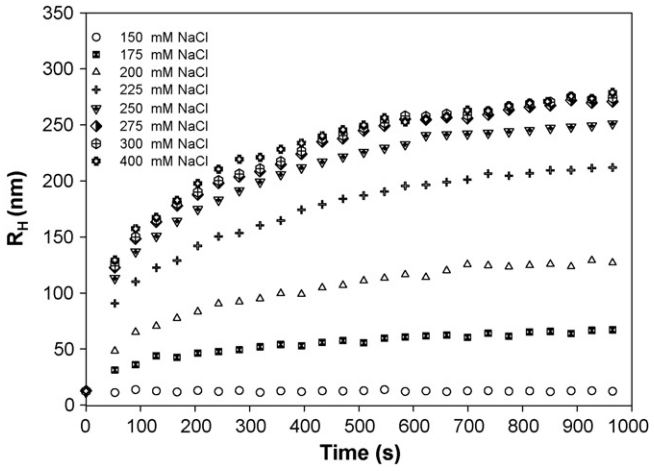

Fig. 1. Hydrodynamic radius of reference nanoparticles measured by dynamic light scattering plotted vs. time for various NaCl concentrations.

concentration (up to 2 M). In fact, the PEG-coated particles were stable in any condition using water as a medium of suspension.

Increasing electrolyte concentrations the slope of the hydrodynamic radius versus time curve increases progressively up to a critical electrolyte concentration, namely critical concentration of coagulation (c.c.c.) as clearly appears in both figures (Romero-Cano et al., 2001). Concentrations higher than c.c.c. superimposed curves with the same slope; this is a clear indication of the fast coagulation state, where the coagulation rate constant is independent of the electrolyte concentration.

The stability ratio W, calculated for each coagulation experiment, was obtained using Eq. (3). The estimation of the slopes of the dR_H/dt curves was possible with a sufficiently accurate solution using a low-order polynomial fitting, even though there was a strong effect of the temporal limit resolution in our samples and curves. The results obtained with NaCl as electrolyte for reference sample and amino-alcohol-coated nanoparticles at two different surface percentages are shown in Fig. 3.

Fig. 3 displays the typical trend with the plateau of the fast aggregation state on the right side. In the slow aggregation

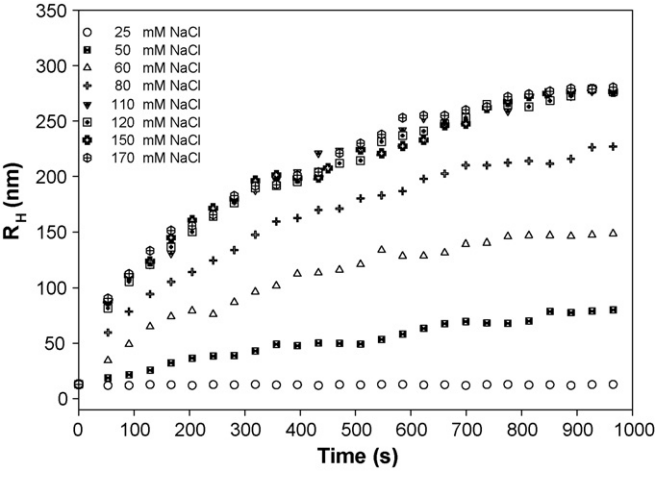

Fig. 2. Hydrodynamic radius of amino-alcohol nanoparticles measured by dynamic light scattering plotted vs. time for various NaCl concentrations.

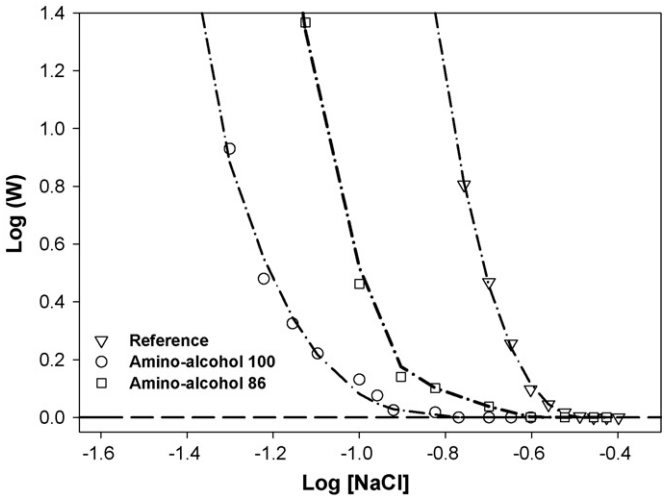

Fig. 3. Colloidal stability curves for reference iron oxide nanoparticles (triangles), amino-alcohol86 coated iron oxide nanoparticles (square) and amino-alcohol100 coated iron oxide nanoparticles (circles). The dash-dot lines are determined from general least squares fitting of the data using Eq. (4) in the text.

region, log W decreases as the salt concentration (ce) increases until the c.c.c. is reached. Adding salt to the dispersion initiates aggregation by suppressing the double-layer repulsion between particles. According to the DLVO, below the c.c.c., the thickness of the electrical double-layer repulsion decreases with increasing salt concentration. The double layer is entirely suppressed above the c.c.c., and the aggregation rate constant is then independent of the salt concentration (rapid aggregation).

Coatings like PEG are usually added to stabilize the colloidal suspensions. If the thickness of the polymer is large enough, the van der Waals attraction between the particles is negligible in comparison to the Brownian thermal energy. This is the origin of the term 'steric' stabilization (Vincent, 1974; Napper, 1977) leading extra repulsive terms in the energy barrier $V_T(H)$. Indeed, even when the double layer is entirely suppressed by the salt concentration, the overlap of polymer layers reduces the volume available to each single chain of polymer, and hence increases dramatically the total energy barrier $V_T(H)$, producing a strong repulsive force between particles (Flory, 1953; Raghavan et al., 2000). Consequently, we found that PEG-coated USPIO particles in water suspension were very stable ($W \approx \infty$). In contrast, the amino-alcohol coating was too small to give rise to significant steric repulsion and it even led to the reduction of the double-layer repulsion between particles. An approximated value of the critical coagulation concentration can be obtained from the relationship between the stability ratio W and the electrolyte concentration (Reerink et al., 1954). In the case of reference iron oxide nanoparticle the c.c.c. value was 270 ± 20 mM (Table 2), for the amino-alcohol-coated system worse values were observed (160 and 120 mM).

The theoretical curves were drawn by fitting the experimental data with Eq. (4), using the Hamaker constant A and the diffusion potential ψ_d as fitting parameters to estimate the steric and electrostatic contributions discussed just above. The A and ψ_d values obtained are shown in Table 2. The values found of the

Table 2
Diffusion potential and Hamaker constant determined from fitting procedure of log W experimental points vs. electrolyte concentration by the Eq. (4) in the text

Kind of coating	ψ_d (mV)	A (10^{-20} J)	c.c.c. (mM)
Reference	-70 ± 3	5.3 ± 0.5	270 ± 30
Amino-alcohol86	-47 ± 2	5.1 ± 0.3	160 ± 20
Amino-alcohol100	-40 ± 2	4.8 ± 0.3	120 ± 20

Hamaker constant have the same magnitude order than those reported in the literature for ferrofluids (Menager et al., 1996; Lalatonne et al., 2004). The diffusion potential values obtained were discussed and related to zeta potential ones below. The A and ψ_d values were directly used to draw the total potential energy of interaction curves ($V_T(H)$) for amino-alcohol-coated and reference nanoparticles (Figs. 4–6). These figures show that

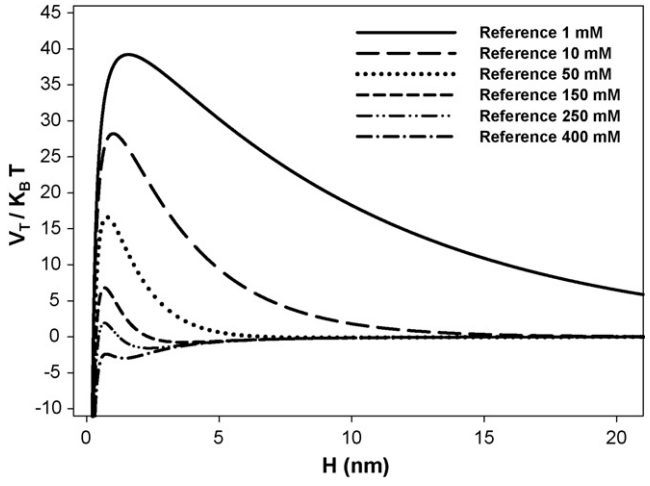

Fig. 4. Calculated total interaction potential ($V_T(H)$ in K_BT units) of reference iron oxide nanoparticles, plotted vs. the distance between the particles (H) for different NaCl concentrations. The Hamaker constant (A) and diffusion potential used values were, respectively, of 5.3×10^{-20} J and -70 mV.

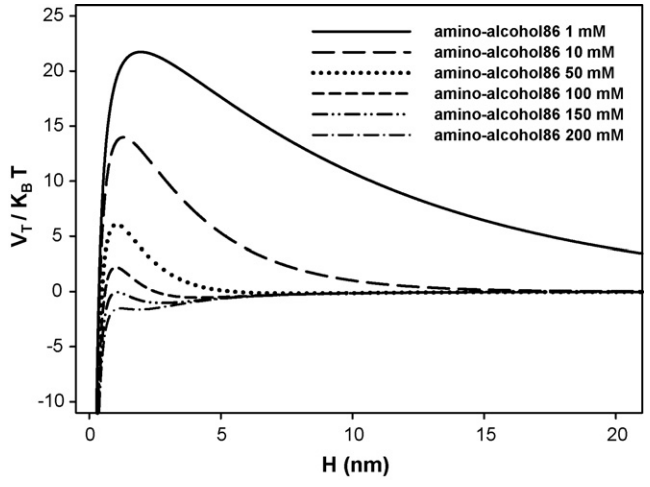

Fig. 5. Calculated total interaction potential ($V_T(H)$ in K_BT units) of amino-alcohol86 coated iron oxide nanoparticles, plotted vs. the distance between the particles (H) for different NaCl concentrations. The Hamaker constant (A) and diffusion potential used values were, respectively, of 5.1×10^{-20} J and -47 mV.

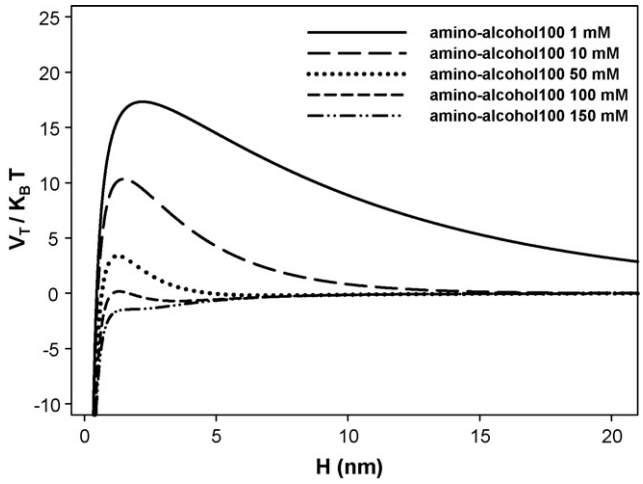

Fig. 6. Calculated total interaction potential ($V_T(H)$ in K_BT units) of amino-alcohol100 coated iron oxide nanoparticles, plotted vs. the distance between the particles (H) for different NaCl concentrations. The Hamaker constant (A) and diffusion potential used values were of 4.8×10^{-20} J and -40 mV.

the stability of the amino-alcohol particles is worse than the stability of reference sample (stabilized only by electrostatic repulsion) and still decreases when the coating percentage is higher. It can be observed in each case that the increase in electrolyte concentration results in a decrease of the potential maximum height. The latter, which prevents aggregation, finally disappears when the electrolyte concentration is similar to the experimental c.c.c. in agreement with the theoretical prediction. It also clearly appears that, for a given salt concentration, the peak level decreases with the lowering of colloidal sample stability. Taking into account, as an example, the curves at 1 mM of NaCl (Figs. 4–6) the peak stands at 40, 22 and 17 ($V_T(H)$ in K_BT units) for reference, amino-alcohol86 and amino-alcohol100, respectively.

The diffusion potential ψ_d value was estimated also by zeta potential ζ (Table 3) determination. Since zeta potential depends on electrolyte concentration, the electrophoretic mobility (μ) was measured versus NaCl concentration (Fig. 7). The electrophoretic mobility at the NaCl concentration of 1 mM was converted to zeta potential (Table 3) using the Smoluchowski and Hückel formula. Table 3 shows the effect of the equation chosen to the zeta potential values. The iron oxide particles used in this study are very small and Hückel formula could be more appropriate than Smoluchowski formula (especially for the reference sample, electrically stabilized). Indeed the zeta potential and diffusion potential are really the same when the particles are uncoated. As expected, for this sample we found the diffusion potential being very close to the zeta potential obtained by Hückel formula (Table 3). The difference between the zeta potential and diffusion potential values observed for the amino-alcohol coatings could be attributed to misuse of the Hückel and Smoluchowski theories since the particles are very small, strongly charged and coated.

Fig. 7 shows the electrophoretic mobility of reference and PEG-coated samples across a range of NaCl concentrations. The measures for amino-alcohol-coated particles were performed at

Table 3
Zeta potential values of the different suspensions obtained by Smoluchowski and Hiickel formulas compared to the diffusion potential determined from fitting procedure of log W experimental points vs. electrolyte concentration by the Eq. (4) in the text

Kind of coating	μ (10^{-8} m^2 s^{-1} V^{-1})	ζ (mV) (Smoluchowski)	ζ (mV) (Hückel)	ψ_d (mV) (fitting)
Reference	−3.77 ± 0.4	−48.1	−72.1	−70
Amino-alcohol86	−3.18 ± 0.4	−40.6	−60.9	−47
Amino-alcohol100	−2.89 ± 0.4	−37.0	−55.0	−40
PEG750	−3.19 ± 0.4	−40.7	−61.1	–
PEG2000	−2.98 ± 0.4	−38.0	−57.0	

NaCl 1 mM (see Table 3), denaturation and aggregation phenomena occurring at higher salt concentration during the course of the experiment.

Fig. 7 shows a rise in electrophoretic mobility, μ (i.e. less negative) as NaCl concentration increases until a plateau is reached. The zeta potential curve shows the same trend regardless of the formula used to convert μ to ζ potential. The charge of PEG-coated nanoparticles is getting much closer to zero than that of the reference sample while these particles remain completely stable, emphasizing the role of steric stabilization in this case. Theoretically, it might be possible to apply the Ohshima equation to estimate the values of the unknown parameters related to the surface characterization (like the softness parameter) of the USPIO particles through a curve-fitting procedure, but in our case it is not possible to find an univocal and physically correct solution. This study illustrates the difficulty of applying the existent theories to particles as small as USPIO especially when trying to evaluate their ζ potential. The use of the original electrophoretic mobility data to characterize the system is surely the most convenient way to minimize misinterpretation. Moreover, the commercially available instruments may be unsuitable for the characterization of size and surface properties of such tiny particles. Indeed the users often encounter problems associated with analytical limits of resolution. A way to overcome these problems could be the combination of different analysis techniques and methods as we recently did with the structural characterization of these USPIO, using two different X-ray diffraction techniques (Di Marco et al., 2006).

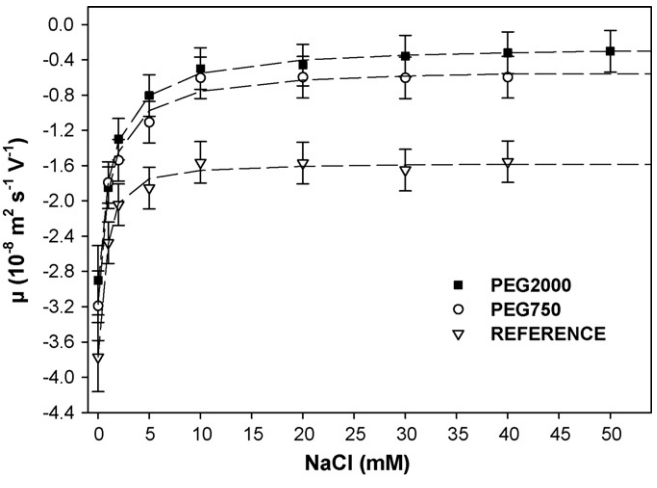

Fig. 7. Electrophoretic mobility vs. NaCl concentration of reference particles (only electrically stabilized by carboxylate) and PEG-coated particles with PEG chains varying by their length (MW ca. 750 and 2000).

Acknowledgements

We would like to thank Dr. I. Raynal, J.-M. Fabicki and A. Dorlain from Guerbet for scientific and technical help, Dr. C. Sadun from University of Rome "La Sapienza" for stimulating conversations, E. Guilbert for helpful suggestion and both the ANRT from the French Ministery and Guerbet S.A. for financial support.

References

Chatterjee, J., Haik, Y., Chen, C., 2003. Size dependent magnetic properties of iron oxide nanoparticles. J. Magn. Mater. 257, 113–118.
Derjaguin, B.V., Landau, L.D., 1941. Theory of the stability of strongly charged lyophobic sols and the adhesion of strongly charged particles in solutions of electrolytes. Acta Physicochim. URSS 14, 633–662.
Di Marco, M., Port, M., Couvreur, P., Dubernet, C., Ballirano, P., Sadun, C., 2006. Structural characterization of ultrasmall superparamagnetic iron oxide (USPIO) particles in aqueous suspension by energy dispersive X-ray diffraction (EDXD). J. Am. Chem. Soc. 128, 10054–10059.
Flory, P.J., 1953. Principles of Polymer Chemistry. Cornell University Press, Ithaca, NY.
Guptaa, A.K., Gupta, M., 2005. Synthesis and surface engineering of iron oxide nanoparticles for biomedical applications. Biomaterials 26, 3995–4021.
Halbreic, A., Roger, J., Pons, J.N., Geldwert, D., Da Silva, M.F., Roudier, M., Bacri, J.C., 1998. Biomedical applications of maghemite ferrofluids. Biochimie 80, 379–390.
Holthoff, H., Egelhaaf, S.U., Borkovec, M., Schurtenberger, P., Sticher, H., 1996. Coagulation rate measurements of colloidal particles by simultaneous static and dynamic light scattering. Langmuir 12, 5541–5549.
Kobayashi, M., Skarba, M., Galletto, P., Cakara, D., Borkovec, M., 2005. Effects of heat treatment on the aggregation and charging of Stöber-type silica. J. Colloid Interface Sci. 292, 139–147.
Kuo, Y.C., Lin, T.W., 2006. Electrophoretic mobility, zeta potential, and fixed charge density of bovine knee chondrocytes, methyl methacrylate-sulfopropyl methacrylate, polybutylcyanoacrylate, and solid lipid nanoparticles. J. Phys. Chem. B 110, 2202–2208.
LaConte, L., Nitin, N., Bao, G., 2005. Magnetic nanoparticle probes. Nanotoday 19, 32–38.
Lalatonne, J., Richardi, J., Pileni, M., 2004. Van der Waals versus dipolar forces controlling mesoscopic organizations of magnetic nanocrystals. Nat. Mater. 3, 121–125.
Menager, C., Belloni, L., Cabuil, V., Dubois, M., Gulik-Krzywicki, T., Zemb, T., 1996. Osmotic equilibrium between an ionic magnetic fluid and an electrostatic lamellar phase. Langmuir 12, 3516–3522.
Moghimi, S.M., Hunter, A.C., Murray, J.C., 2001. Pharmacol. Rev. 53, 283–318.
Mornet, S., Vasseur, S., Grasset, F., Duguet, E., 2004. Magnetic nanoparticle design for medical diagnosis and therapy. J. Mater. Chem. 14, 2161–2175.
Napper, D.H., 1977. Steric stabilization. J. Colloid Interface Sci. 58, 390–407.

Ohshima, H., 1995. Electrophoresis of soft particles. Adv. Colloid Interface Sci. 62, 189–235.

Ortega-Vinuesa, J.L., Martin-Rodriguez, A., Hidalgo-Alvarez, R., 1996. Colloidal stability of polymer colloids with different interfacial properties: mechanisms. J. Colloid Interface Sci. 184, 259–267.

Overbeek, J.T.G., 1982. Monodisperse colloidal systems, fascinating and useful. Adv. Colloid Interface Sci. 15, 251–277.

Pouliquen, D., Perroud, H., Calza, F., Jallet, P., Le Jeune, J.J., 1992. Investigation of the magnetic properties of iron oxide nanoparticles used as contrast agent for MRI. Magn. Reson. Med. 24, 75–84.

Port, M., Corot, C, Raynal I., Rousseaux, O, 2004. Novel compositions magnetic particles. Patent no. US2,004,253,181. December 16.

Puertas, A.M., de las Nieves, F.J., 1999. Colloidal stability of polymer colloids with variable surface charge. J. Colloid Interface Sci. 216, 221–229.

Raghavan, S.R., Hou, J., Baker, G.L., Khan, S.A., 2000. Colloidal interactions between particles with tethered nonpolar chains dispersed in polar media: direct correlation between dynamic rheology and interaction parameters. Langmuir 16, 1066–1077.

Reerink, H., Overbeek, J., Th., G., 1954. The rate of coagulation as a measure of the stability of silver iodide sols. Discuss. Faraday Soc. 18, 74–84.

Romero-Cano, M.S., Martin-Rodriguez, A., de las Nieves, F.J., 2001. Electrosteric stabilization of polymer colloids with different functionality. Langmuir 17, 3505–3511.

Schudel, M., Behrens, S.H., Holthoff, H., Kretzschmar, R., 1997. Absolute aggregation rate constants of hematite particles in aqueous suspensions: A comparison of two different surface morphologies. J. Colloid Interface Sci. 196, 241–253.

Tartaj, P., Morales, M.P., Veintemillas-Verdaguer, S., Gonzalez-Carreño, T., Serna, C., 2005. Advances in magnetic nanoparticles forbiotechnology applications. J. Magn. Magn. Mater. 290–291, 28–34.

Vervey, E.J.W., Overbeek, J.Th.G., 1948. Theory of Stability of Lyophobic Colloids. Elsevier, Amsterdam.

Vincent, B., 1974. The effect of adsorbed polymers on the stability of dispersions. Adv. Colloid Interface Sci. 4, 193–277.